AIMS Materials Science, 10(5): 891–908.
DOI: 10.3934/matersci.2023048
Received: 24 July 2023
Revised: 11 September 2023
Accepted: 19 September 2023
Published: 12 October 2023

http://www.aimspress.com/journal/Materials

Research article

Investigating parametric homogenization models for natural frequency of FGM nano beams

Abdelhak Berkia[1], Billel Rebai[2,*], Bilal Litouche[3], Soufiane Abbas[4] and Khelifa Mansouri[1,5]

[1] Faculty of Sciences & Technology, Mechanical Eng Department, University Abbes Laghrour Khenchela, Algeria
[2] Faculty of Sciences & Technology, Civil Eng Department, University Abbes Laghrour Khenchela, Algeria
[3] Mechanic and Electro-Mechanic Department, University Center Abdelhafid Boussouf, Mila, Algeria
[4] LMRS Laboratory, Faculty of Technology, University of Sidi Bel Abbes, Algeria
[5] Laboratory of Eng and Sciences of Advanced Materials (ISMA), Khenchela, Algeria

*** Correspondence:** Email: billel.rebai@univ-khenchela.dz; Tel: +213-055-019-6631.

Abstract: This research focuses on exploring the free vibration behavior of functionally graded (FG) nano-beams. To calculate the effective properties of the FG nano-beam, which varies solely in the thickness direction, the four homogenization schemes Mori-Tanaka, Tamura, Reuss and Voigt are employed. This study employs high-order shear deformation nano-beam theory and derives the governing equations of motion using nonlocal differential constitutive relations of Eringen. Hamilton's principle is utilized in conjunction with the refined three variables beam theory. The consideration of a length scale parameter accounts for small-scale effects. Analytical solutions are obtained for a simply supported FG nano-beam and compared with existing literature solutions. The research also investigates the influence of different homogenization schemes, the nonlocal parameter, beam aspect ratio and various material compositions on the dynamic response of the FG nano-beam.

Keywords: Hamilton's principle; length scale parameter; Eringen theory; free vibration; homogenization models; nano-beams

1. Introduction

Nano-beam materials are composites made up of nanotubes, nanowires and nanoparticles which are manipulated on a nanoscale level and used in a variety of applications. Researchers have utilized Eringen's nonlocal elasticity theory to investigate the static deformation, free vibration, bending, buckling and wave properties of nano-beams and other structures like nano-plates and curved nano-shells [1–3].

Recent research on nanobeam functionally graded beams has gained traction, with various studies conducted to explore the current state of this field. This discussion provides an in-depth analysis of the published articles, offering insight into potential applications of this technology. By examining current trends, potential improvements and applications, this research can help to further our understanding of nanobeam functionally graded beams and their utility. In their study, Vinh and Tounsi [4] investigated the free vibration of functionally graded doubly curved nanoshells using nonlocal first-order shear deformation theory. They compared the frequencies obtained to existing results and examined the effects of nonlocal parameters and the power-law index on the nanoshells. Additionally, in their later work [5] they determined the effect of a spatial variation in the nonlocal parameter on the free vibration of functionally graded sandwich (FGSW) nanoplates, finding that the natural frequencies were significantly reduced. Cuong-Le et al. investigated the linear and nonlinear solutions of a sigmoid functionally graded material nanoplate with porous effects, using isogeometric finite element formulation to examine the effects of power indexes, aspect ratios, nonlocal and strain gradient parameters [6]. Liu et al. sought to understand the dynamic deflection response of an exponentially functionally graded material (E-FGM) nanoplate embedded in a visco-elastic foundation when subjected to a moving load, utilizing third-order shear deformation theory, Eringen nonlocal elasticity and a state-space method to analyze the influence of nonlocality, volume fraction index, porosity index, visco-elastic foundation coefficients and velocity and time span of a moving load on the forced vibration of the nanoplate [7]. Faghidian and Tounsi studied wave dispersion and free vibrations of elastic nano-beams through the mixture unified gradient theory, providing insight into the augmented elasticity theory's effectiveness in softening and stiffening responses [8]. John Peddieson utilized nonlocal elasticity theory to develop a nonlocal Benoulli/Euler beam model for cantilever beams [9], and Xu Mingtian [10] applied the same theory in combination with an integral equation approach to investigate the free transverse vibrations of nano-to-micron scale beams. Rebai Billel has studied the effects of homogenization models on the stress, deflection and vibration behavior of functionally graded plates subjected to thermal and mechanical loads [11–13]. Reddy et al. have evaluated the static bending, vibration, and buckling responses of beams with various boundary conditions using nonlocal differential constitutive relations of Eringen. They have presented analytical solutions and numerical results to show the effect of nonlocal behavior on deflections, buckling loads and natural frequencies of beams [14,15]. Zhang and Qing introduced well-posed two-phase nonlocal models for nanobeam vibrations based on higher-order shear deformation theory. Their work also encompassed the examination of refined shear deformation beams' buckling behavior under thermal loading [16]. Additionally, Zhang, Schiavone and Qing extended their research to encompass hygro-thermal vibration analysis of nanobeams. This analysis employed stress-driven nonlocal theory and incorporated two-variable shear assumptions [17,18]. Ebrahimi has examined the vibration characteristics of magneto-electro-thermo-elastic functionally graded nano-beams in the framework of third order shear deformation theory [19], while Thai et al. have presented a nonlocal sinusoidal shear deformation beam

theory for the bending, buckling and vibration of nano-beams [20]. Eltaher et al. have conducted a free vibration analysis of size-dependent functionally graded nano-beams using the finite element method based on the nonlocal continuum model of Eringen [21] and Nazemezhad et al. have investigated the nonlinear free vibration of functionally graded nano-beams with immovable ends using nonlocal elasticity and Euler-Bernoulli beam theory [22]. Ebrahimi has studied the static stability and free vibration characteristics of functionally graded nano-beams using a nonlocal couple stress theory [23]; Hadji et al. have investigated the free vibration of porous functionally graded nano-beams using a new nonlocal hyperbolic shear deformation beam theory [24]; Youcef et al. have focused on the behavior of non-local shear deformation beam theory for the vibration of functionally graded (FG) nano-beams with porosities [25]; and Shariati et al. have examined the size-dependent vibrations and stability of axially functionally graded (AFG) nano-beams using a nonlocal elasticity theory [26].

Other research conducted by Cornacchia et al. delved into the analytical solutions pertaining to the linear vibrations and buckling of nano plates [27]. Following suit, Tocci Monaco et al. conducted an in-depth investigation into the critical temperatures associated with magneto-electro-elastic nonlocal strain gradient plates [28]. Luciano et al. contributed significantly by exploring free flexural vibrations in nanobeams with non-classical boundary conditions [29]. Additionally, Fabbrocino et al. made substantial strides in the field with their research on dynamic crack growth utilizing a moving mesh method. These research endeavors collectively offer invaluable insights and research findings, advancing the knowledge base in these areas of study [30].

Several researchers have examined the oscillations, bending and buckling effects, vibration characteristics, static and dynamic characteristics and nonlinear bending of power functionally graded micro plate (PFGM) microplates, microbeams, nano-beams and elasto-plastic beams based on the classical beam theory, modified couple stress theory, Euler-Bernoulli beam kinematic theory, non-local elasticity theory, higher-order shear beam deformation theories, strain gradient theory and Bernoulli-Euler beam model, respectively [31–46].

In recent findings by Wu et al. on dynamics of nanostructures including vibrations in graphene sheets and nanobeams, this work validates computational models for accurate prediction of natural frequencies across a wide parameter space [47,48].

B. Karami et al. investigated the free vibration behavior of a curved microbeam composed of a functionally graded material (FGM) using the modified strain gradient theory of elasticity and first-order shear deformation theory. In the study, various homogenization models, such as Voigt, Reuss, Hashin-Shtrikman bounds and cubic local representative volume elements (LRVE) schemes were employed to determine the effective material properties of the FGM curved microbeam [49].

Compared to earlier investigations using simple models like Euler-Bernoulli beam theory, current research utilizes more advanced approaches like higher-order shear deformation theory and isogeometric finite element formulation to capture complex behaviors of functional nanobeams. Advantages include analyzing complex geometries, deflections, porosities and foundations for practicable insight. Challenges remain around computational efficiency for real applications. Overall trends point to a focus on novel materials, geometries and theories to progress functional nanobeam research toward utilization through solving practical engineering problems.

This research uses the Mori-Tanaka, Tamura, Reuss and Voigt homogenization schemes and the high-order shear deformation nano-beam theory to derive the governing equations of motion using Hamilton’s principle and the nonlocal differential constitutive relations of Eringen. Analytical solutions are then obtained from this data and compared with other solutions in the literature. The

effects of the various homogenization schemes, nonlocal parameter, beam aspect ratio and material compositions on the dynamic response of the FG nano-beam are also investigated. This study undertakes a first-of-its-kind comparative vibration analysis of FGM nano-beams using four homogenization techniques and comprehensive parametric study of nonlocal parameters, gradient indices, volume fractions and geometries. This work provides new insights into the natural frequencies and mode shapes. The comparative homogenization scheme analysis and extensive vibrational behavior investigation pave the way for optimized design and future stability, buckling and wave propagation studies of FGM nano-beams.

2. Nano-beam with different homogenization schemes

Figure 1 shows FG nano-beam of length *L*, width *b* and thickness *h*. The material on the top surface ($z = +h/2$) of the plate is ceramic and is graded to metal at the bottom surface of the plate ($z = -h/2$).

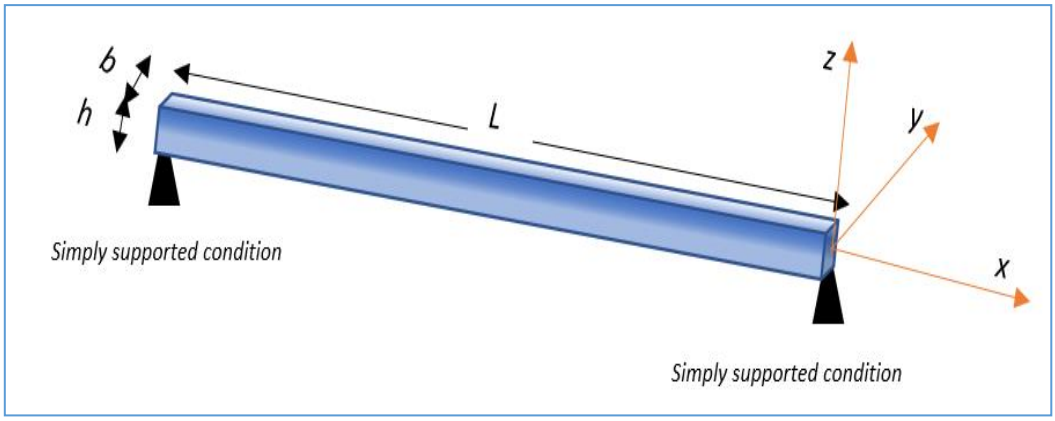

Figure 1. The geometry domain of the FG nano-beam.

The volume distribution fraction through the thickness has been identified as the following function, using Eq 1, where *p* is the material index.

$$V(z) = \left(\frac{2z+h}{2h}\right)^{p} \tag{1}$$

The micromechanics models chosen for the comparison study are detailed in sections 2.1. to 2.4.

2.1. Mixture law (Voigt model)

Mixture law, also known as the Voigt model, is a mathematical model that describes the behavior of a composite material. It assumes that the properties of the composite material are obtained by combining the properties of the individual components in a linear manner. It is used to calculate the effective modulus of elasticity, strength and other properties of a composite material using Eq 2 [50].

$$P(z) = P_c V(z) + P_m\big(1 - V(z)\big) \tag{2}$$

2.2. Reuss model

The Reuss model is a mathematical model used to calculate the effective properties of a composite material. It assumes that the properties of the composite material are obtained by averaging the properties of the individual components. It is used to calculate the effective modulus of elasticity, strength and other properties of a composite material. Eq 3 calculates the proprieties of FG structures with the assumption that the stress is uniform through the thickness [51].

$$P(z) = \frac{P_c P_m}{P_c(1-V(z))+P_m V(z)} \tag{3}$$

2.3. Tamura model

The Tamura model is a mathematical model used to calculate the effective properties of a composite material. It is based on the concept of strain energy density and assumes that the properties of the composite material are obtained by combining the properties of the individual components in a non-linear manner. It is used to calculate the effective modulus of elasticity, strength and other properties of a composite material using Eq 4 [52].

The method of Tamura is another way to express the linear law of Voigt where the empirical term q "stress-to-strain transfer" has been added in formulation [53].

$$P(z) = \frac{(1-V(z))\,P_m(q\ -P_c)+V(z)\,P_c}{P_c(1-V(z))+P_m V(z)(1-V(z))\,(q\ -P_c)+V(z)\,P_c(q-P_m)} \tag{4}$$

2.4. Mori-Tanaka model

The Mori-Tanaka method is a homogenization scheme used to estimate the effective properties of FGM. This method was developed by Mori and Tanaka in 1973 and is based on the assumption that the material properties in the microstructure can be represented by a representative volume element (RVE). The method uses small strain theory and assumes that the RVE is composed of an assembly of small particles of different materials which interact through elasticity. The Mori-Tanaka method can also be used to calculate the effective thermal conductivity and effective electrical conductivity of the FGM using Eq 5 [54].

The Mori-Tanaka homogenization scheme formulation is given by [55–58]:

$$P(z) = P_m + \frac{V(z)\,(P_c-P_m)}{1+\frac{(1-V(z))(3P_c-P_m)}{3P_m+4}} \tag{5}$$

where *P(z)* is the effective material property. *Pm* and *Pc* are the properties of the metal and ceramic faces of the beam respectively.

3. Kinematics

The displacement field of the current theory is based on the assumption that in-plane and transverse displacements are split into bending and shear components, that bending parts of in-plane displacement are similar to d'Euler Bernoulli theory and that shear parts of in-plane displacement

induce hyperbolic variations of shear strains and shear stresses which vanish on the top and bottom surfaces of the beam. Those result in the following displacement field, as shown in Eq 6:

$$\begin{gathered} u(x,z,t) = u_0(x,t) - z\frac{\partial w_b}{\partial x} + f(z)\frac{\partial w_s}{\partial x} \\ w(x,z,t) = w_b(x,t) + w_s(x,t) \end{gathered} \tag{6}$$

Here, $u_0(x,t)$ denotes the displacements along the x coordinate directions of a point on the mid-plane of the beam; $w_b(x,t)$and $w_s(x,t)$ are the bending and shear components of the transverse displacements, respectively. The nonzero strains associated with the displacement field are shown in Eq 7:

$$\varepsilon_x = \varepsilon_x^0 + zk_x^b + f(z)k_x^s \text{ et } \gamma_{xz} = g(z)\gamma_{xz}^s \tag{7}$$

where: $\varepsilon_x^0 = \frac{\partial u_0}{\partial x}$, $k_x^b = -\frac{\partial^2 w_b}{\partial x^2}$, $k_x^s = -\frac{\partial^2 w_s}{\partial x^2}$, $\gamma_{xz}^s = \frac{\partial w_s}{\partial x}$, $f(z) = \frac{-1}{4}z + \frac{5}{3}z\left(\frac{z}{h}\right)^2$, $g = \frac{5}{4} - 5\left(\frac{z}{h}\right)^2$.

4. Constitutive relations

The nonlocal constitutive relation for the macroscopic stress takes the following form, as shown in Eq 8:

$$\begin{gathered} \sigma_x - \mu\frac{d^2\sigma_x}{dx^2} = E\varepsilon_x \\ \tau_{xz} - \mu\frac{d^2\tau_{xz}}{dx^2} = G\gamma_{xz} \end{gathered} \tag{8}$$

where E and G are Young's modulus and shear modulus, respectively. Moreover, e_0 is a material constant, and a is the internal characteristic length. Once the nonlocal parameter $\mu = (e_0 a)^2$ is equal to zero, we obtain the constitutive relations of the local theories.

5. Equations of motion

Hamilton's principle is used herein to derive the equations of motion. We have obtained:

$$\int_0^L \int_A (\sigma_x \delta\varepsilon_x + \tau_{zx}\delta\gamma_{zx})dAdx - \int_0^L \int_A \rho[\ddot{u}_0\delta u_0 + (\ddot{w}_b + \ddot{w}_s)\delta(w_b + w_s)]dAdx = 0 \tag{9}$$

Integrating by parts Eq 9, and collecting the coefficients of δu_0, $\delta w_b$and δw_s, the following equations of stability are obtained by Eq 10:

$$\begin{gathered} \delta u_0 : \frac{dN}{dx} = I_0\ddot{u}_0 \\ \delta w_b : \frac{d^2M_b}{dx^2} = I_0(\ddot{w}_b + \ddot{w}_s) - I_2\frac{d^2\ddot{w}_b}{dx^2} \\ \delta w_s : \frac{d^2M_s}{dx^2} + \frac{dQ}{dx} = I_0(\ddot{w}_b + \ddot{w}_s) - \frac{I_2}{84}\frac{d^2\ddot{w}_s}{dx^2} \end{gathered} \tag{10}$$

where N, M_b, M_s and Q are stress resultants and they are defined by:

$$(N, M_b, M_s) = \int_A (1, z, f)\sigma_x dA \tag{11}$$

$$Q = \int_A g\tau_{xz} dA \tag{12}$$

And (I_0, I_2) are mass inertias defined as:

$$(I_0, I_2) = \int_A (1, z^2)\rho(z) dA \tag{13}$$

Substituting Eqs 11–13 into Eq 8 and integrating through the thickness of the beam, the stress resultants are related to the generalized displacements by the relations:

$$\begin{aligned} N - \mu\frac{d^2N}{dx^2} &= A\frac{du_0}{dx} - B\frac{d^2w_b}{dx^2} - B_s\frac{d^2w_s}{dx^2} \\ M_b - \mu\frac{d^2M_b}{dx^2} &= B\frac{du_0}{dx} - D\frac{d^2w_b}{dx^2} - D_s\frac{d^2w_s}{dx^2} \\ M_s - \mu\frac{d^2M_s}{dx^2} &= B\frac{du_0}{dx} - D\frac{d^2w_b}{dx^2} - H_s\frac{d^2w_s}{dx^2} \\ Q - \mu\frac{d^2Q}{dx^2} &= A_s\frac{dw_s}{dx} \end{aligned} \tag{14}$$

where: $\{A, B, D, \bar{E}, F, H\} = \int_A \{1, z, z^2, z^3, z^4, z^6\}E(z)dA$, $B_s = -\frac{1}{4}B + \frac{5}{3h^2}\bar{E}$, $D_s = -\frac{1}{4}D + \frac{5}{3h^2}F$, $H_s = \frac{1}{16}D - \frac{5}{6h^2}F + \frac{25}{9h^4}H$, $\{A_{55}, D_{55}, F_{55}\} = \int_A \{1, z^2, z^4\}G(z)dA$, $A_s = \frac{25}{16}A_{55} - \frac{25}{2h^2}D_{55} + \frac{25}{h^4}F_{55}$.

Substituting from Eq 14 into Eq 8, we obtain the following equation in terms of (u_0, w_b, w_s):

$$\begin{aligned} A\frac{d^2u_0}{dx^2} - B\frac{d^3w_b}{dx^3} - B_s\frac{d^3w_s}{dx^3} &= I_0\left(\ddot{u}_0 - \mu\frac{d^2\ddot{u}_0}{dx^2}\right) \\ B\frac{d^3u_0}{dx^3} - D\frac{d^4w_b}{dx^4} - D_s\frac{d^4w_s}{dx^4} &= I_0\left((\ddot{w}_b + \ddot{w}_s) - \mu\frac{d^2(\ddot{w}_b + \ddot{w}_s)}{dx^2}\right) - I_2\left(\frac{d^2\ddot{w}_b}{dx^2} - \mu\frac{d^4\ddot{w}_b}{dx^4}\right) \\ B_s\frac{d^3u_0}{dx^3} - D_s\frac{d^4w_b}{dx^4} - H_s\frac{d^4w_s}{dx^4} + A_s\frac{d^2w_s}{dx^2} &= I_0\left((\ddot{w}_b + \ddot{w}_s) - \mu\frac{d^2(\ddot{w}_b + \ddot{w}_s)}{dx^2}\right) - \frac{I_2}{84}\left(\frac{d^2\ddot{w}_s}{dx^2} - \mu\frac{d^4\ddot{w}_s}{dx^4}\right) \end{aligned} \tag{15}$$

6. Exact solution for a simply-supported FG beam

Following the Navier solution procedure, we assume the solution form for u_0, w_b,w_s that satisfies simply-supported FG conditions.

$$\begin{Bmatrix} u_0 \\ w_b \\ w_s \end{Bmatrix} = \sum_{m=1}^{\infty} \begin{Bmatrix} U_n\cos(\alpha x)e^{i\omega t} \\ W_{bn}\sin(\alpha x)e^{i\omega t} \\ W_{sn}\sin(\alpha x)e^{i\omega t} \end{Bmatrix} \tag{16}$$

where U_n,W_{bn} and W_{sn} are arbitrary parameters to be determined, ω is the eigen-frequency associated with (n)th eigen-mode.

Substituting Eq 16 into Eq 15, the analytical solutions can be obtained from the Eq 17:

$$\left(\begin{bmatrix} A\alpha^2 & -B\alpha^3 & -B_s\alpha^3 \\ -B\alpha^3 & D\alpha^4 & D_s\alpha^4 \\ -B_s\alpha^3 & D_s\alpha^4 & H_s\alpha^4 + A_s\alpha^2 \end{bmatrix} - (1+\mu\alpha^2)\omega^2 \begin{bmatrix} I_0 & -I_1\alpha & -J_1\alpha \\ -I_1\alpha & I_0 + I_2\alpha^2 & I_0 + J_2\alpha^2 \\ -J_1\alpha & I_0 + J_2\alpha^2 & I_0 + K_2\alpha^2 \end{bmatrix}\right)\begin{Bmatrix} U_n \\ W_{bn} \\ W_{sn} \end{Bmatrix} = \begin{Bmatrix} 0 \\ 0 \\ 0 \end{Bmatrix} \quad (17)$$

7. Numerical results and discussion

This section compares the proposed homogenization model with the one published by Zemri et al. [59] in order to verify the accuracy of different homogenization models (Reuss, Tamura and Mori-Tanaka). It also provides a parametric analysis of the effects of the nonlocal parameter, the material index, the length-to-thickness ratio and the type of phases constituting the FGM nano-beam on its natural frequency.

7.1. Comparisons and validation

The Tanaka, Tamura, and Reuss model was compared to and validated with the Voigt model used by Zemri et al. [59] to ensure the accuracy of the results. The material properties of the FGM nano-beams, consisting of six different combinations of stainless steel (SUS304) and aluminum (Al) with either zirconia (ZrO_2), aluminia (Al_2O_3) or silicon carbide (SiC), are shown in Table 1. These combinations are named FGM1–1 SUS304/ZrO_2, FGM1–2 SUS304/Al_2O_3, FGM1–3 SUS304/SiC, FGM2–1 Al/ZrO_2, FGM2–2 Al/Al_2O_3 and FGM2–3 Al/SiC FGM nano-beams, respectively.

Table 1. Material properties of metal and ceramic.

	Young's modulus (GPa)	Mass density (kg/m^3)	Poisson' sratio
Stainless steel (SUS304)	210	7800	0.3
Aluminum (Al)	70	2702	0.3
Airconia (ZrO_2)	151	3000	0.3
Aluminia (Al_2O_3)	380	3800	0.3
Silicon carbide (SiC)	420	3210	0.3

In all cases, we present the non-dimensional frequency defined as shown in Eq 18:

$$\bar{\omega} = \omega L^2 \sqrt{\frac{\rho_c A}{E_c I}} \quad (18)$$

Tables 2 and 3 provide a comprehensive comparison of the fundamental frequency of nano-beams for the four different models: Voigt, Tanka, Tamura and Reuss. The varying length-to-thickness ratios and material indices of the nonlocal parameter indicate that the results are reliable and accurate. The validation results show good agreement across the different models, demonstrating the trustworthiness of the models.

7.2. Parametric study

7.2.1. Effect of the length-to-thickness ratio the FGM nano beam on its natural frequency

Figure 2 demonstrates the variation in the natural frequency of an FGM nano beam when evaluated using four homogenization models (Voigt, Tamura, Tanak and Reuss) with a length-to-thickness ratio of 10 to 100, material index of 1 and a nonlocal parameter of 4.

It can be seen from Figure 2 that the natural frequency of the FGM nano-beam increases with the length-to-thickness ratio l for all four homogenization models. As the l/h ratio increases, the beam becomes longer and thinner, resulting in an increase in natural frequency. It is also notable that the Reuss and Tamura models provide the same natural frequency values, while the Voigt and Tanak models give lower values. This discrepancy is due to the assumptions made in each model. Furthermore, the relative difference between the natural frequency evaluated using the four homogenization models decreases as the length-to-thickness ratio increases, albeit only slightly The relative difference = [ω(Reuss) – ω(Voigt, Tamura, Tanak)]/ω(Reuss) between the natural frequency of the FGM nano-beam evaluated using the four homogenization models is 0.059 when l is 10 and 0.038 when l is 100.

7.2.2. Effect of the nonlocal parameter the FGM nano-beam on its natural frequency

Figure 3 shows how the natural frequency of an FGM nano-beam changes as the nonlocal parameter ranges from 0 to 5, while keeping the material index at 1 and length-to-thickness ratio at 10, when evaluated using four different homogenization models (Voigt, Tamura, Tanak and Reuss).

The data in Figure 3 displays that, as the nonlocal parameter increases from 0 to 5, the natural frequency of an FGM nano-beam decreases and the Tanak model gives the lowest frequency value. Among the models, the Voigt model shows the most pronounced decrease in natural frequency, dropping from 6.881 to 5.630 (a decrease of 1.251). The Tanak model shows a decrease of 1.231 from 6.625 to 5.394. The Tamura and Reuss models show a decrease of 0.707 from 7.004 to 6.297. This decrease in frequency is due to the nonlocal parameter making the beam stiffer, which in turn reduces its natural frequency. The larger the nonlocal parameter, the more rigid the beam becomes and thus the lower the frequency.

7.2.3. Effect of the material index of the FGM nano-beam on its natural frequency

Figure 4 presents the natural frequency of an FGM nano-beam evaluated with four homogenization models (Voigt, Tamura, Tanak and Reuss) when the material index p is changed from 0 to 30, and length-to-thickness ratio and nonlocal parameter are both kept at 10 and 4, respectively.

The natural frequency decreases as the material index increases in Figure 4. The Tanak model produces the smallest values of natural frequency, which means that the nano-beam is the most flexible when evaluated with this model.

Table 2. Fundamental frequency of nano-beams for different scheme's models with varying length-to-thickness ratios, material index and nonlocal parameters.

l/h	*p*	0				0.5				1			
		Zemri	Tanaka	Tamura	Reuss	Zemri	Tanaka	Tamura	Reuss	Zemri	Tanaka	Tamura	Reuss
10	0	9.7075	9.7075	9.7075	9.7075	9.5899	9.5899	9.5899	9.5899	9.2612	9.2612	9.2612	9.2612
	1	6.8814	6.6246	7.0040	7.0040	6.7981	6.5444	6.9192	6.9191	6.5651	6.3201	6.6820	6.6820
	3	6.0755	5.9100	6.1186	6.1185	6.0019	5.8384	6.0444	6.0444	5.7962	5.6383	5.8373	5.8373
	10	5.5768	5.4494	5.5425	5.5425	5.5092	5.3834	5.4754	5.4754	5.3204	5.1989	5.2877	5.2877
30	0	9.8511	9.8510	9.8510	9.8510	9.8376	9.8376	9.8376	9.8376	9.7975	9.7975	9.7975	9.7975
	1	6.9832	6.7265	7.1113	7.1113	6.9737	6.7173	7.1016	7.1015	6.9452	6.6899	7.0726	7.0726
	3	6.1712	6.0038	6.2162	6.2161	6.1627	5.9956	6.2077	6.2076	6.1376	5.9711	6.1823	6.1823
	10	5.6655	5.5340	5.6290	5.6290	5.6578	5.5264	5.6213	5.6213	5.6347	5.5039	5.5984	5.5984
100	0	9.8679	9.8679	9.8679	9.8679	9.8667	9.8667	9.8667	9.8667	9.8631	9.8631	9.8630	9.8630
	1	6.9952	6.7384	7.1239	7.1239	6.9943	6.7376	7.1230	7.1230	6.9917	6.7351	7.1204	7.1204
	3	6.1824	6.0148	6.2276	6.2276	6.1817	6.0140	6.2269	6.2268	6.1794	6.0118	6.2246	6.2245
	10	5.6759	5.5439	5.6392	5.6391	5.6752	5.5432	5.6385	5.6385	5.6731	5.5411	5.6364	5.6364

Table 3. Fundamental frequency of nano-beams for different scheme's models with varying length-to-thickness ratios, material index and nonlocal parameters.

l/h	*p*	1.5				2			
		Zemri	Tanaka	Tamura	Reuss	Zemri	Tanaka	Tamura	Reuss
10	0	8.7813	8.7813	8.7813	8.7813	8.2197	8.2197	8.2197	8.2196
	1	6.2249	5.9926	6.3357	6.3357	5.8267	5.6093	5.9305	5.9305
	3	5.4959	5.3462	5.5348	5.5348	5.1443	5.0042	5.1808	5.1808
	10	5.0447	4.9295	5.0137	5.0137	4.7221	4.6142	4.6930	4.6930
30	0	9.7318	9.7318	9.7317	9.7317	9.6419	9.6418	9.6419	9.6418
	1	6.8987	6.6450	7.0252	7.0251	6.8349	6.5836	6.9603	6.9603
	3	6.0964	5.9310	6.1409	6.1408	6.0401	5.8763	6.0841	6.0841
	10	5.5969	5.4669	5.5608	5.5608	5.5452	5.4164	5.5095	5.5094
100	0	9.8570	9.8570	9.8570	9.8569	9.8485	9.8485	9.8485	9.8485
	1	6.9874	6.7310	7.1160	7.1160	6.9814	6.7252	7.1099	7.1099
	3	6.1756	6.0081	6.2207	6.2207	6.1703	6.0030	6.2154	6.2153
	10	5.6697	5.5377	5.6329	5.6329	5.6648	5.5330	5.6281	5.6280

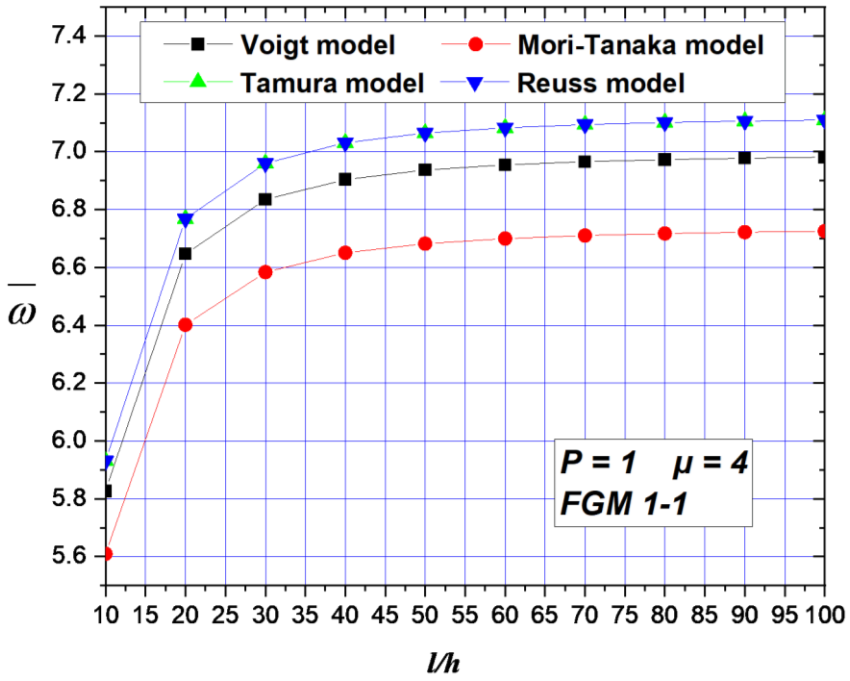

Figure 2. Variation of natural frequency of FGM nano-beam with different length-to-thickness ratios (P = 1, μ = 4, FGM 1–1).

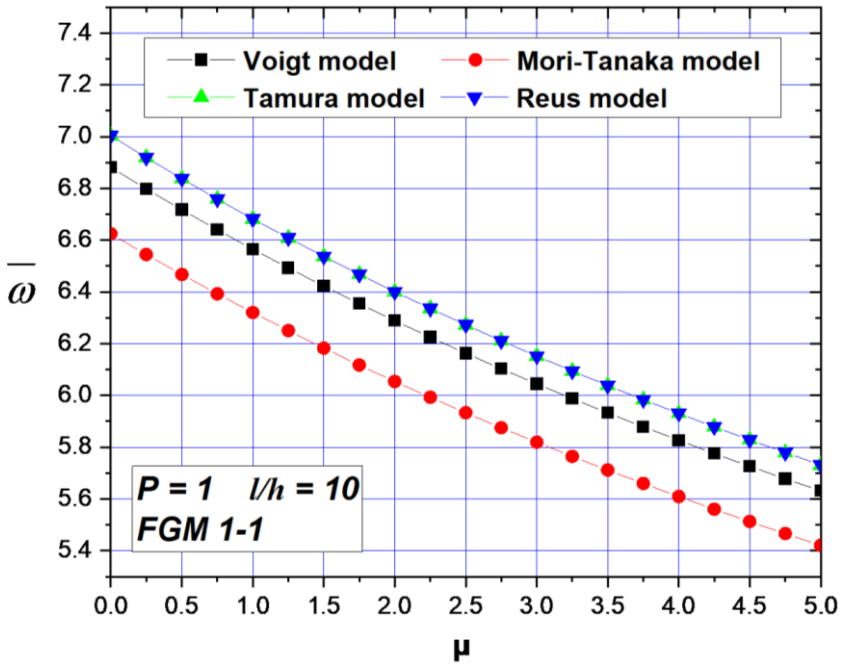

Figure 3. Variation of natural frequency of an FGM nano-beam with nonlocal parameter (P = 1, *l*/*h* = 10).

7.2.4. Effect of type of phases constituting the FGM nano-beam on its natural frequency

In this section, the impact of various metal and ceramic material combinations on the natural frequency of an FGM nano-beam is studied through a parametric analysis. The figure depicts the natural frequency of FGM nano-beams composed of six different combinations of stainless steel (SUS304) and aluminum (Al) with either zirconia (ZrO_2), aluminia (Al_2O_3) or silicon carbide (SiC). The frequency is calculated using the Reuss model with different *l*/*h* ratios, ranging from 10 to 100, a material index of 1 and a nonlocal parameter of 4.

As shown in Figure 5, the length-to-thickness ratio (*l*/*h*) has a crucial impact on the natural frequency of FGM nano-beams. As *l*/*h* increases, the natural frequency of the FGM nano-beams also increases. In this figure, FGM12 SUS304/Al_2O_3 has the highest natural frequency among the FGM nano-beams due to its high elastic modulus and low density compared to other FGM nano-beams. Conversely, FGM2–3 Al/SiC has the lowest natural frequency due to its low elastic modulus and high density. It is evident that the natural frequency of FGM nano-beams is greatly influenced by both their length-to-thickness ratio (*l*/*h*) and material properties.

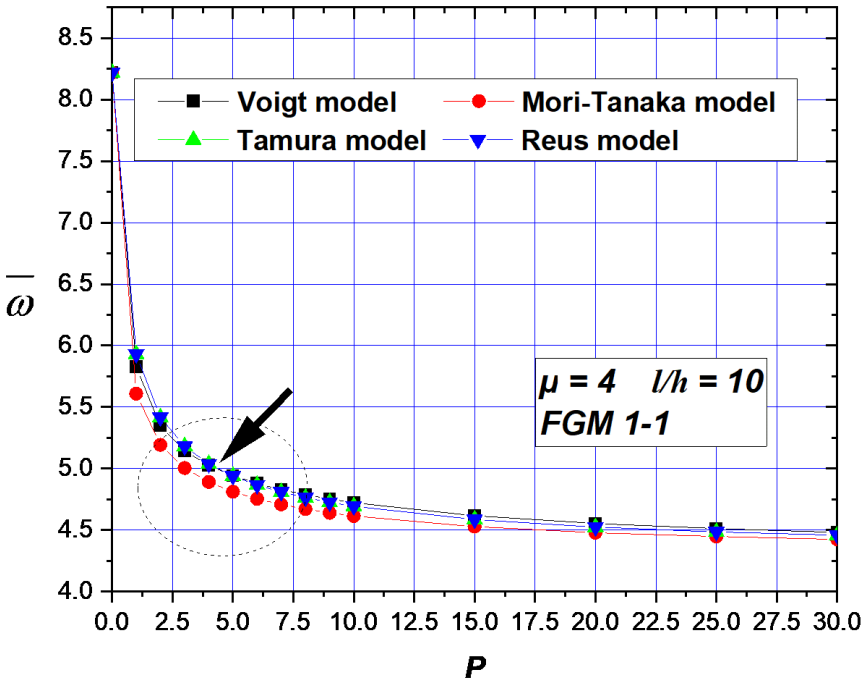

Figure 4. Variation of natural frequency of an FGM nano-beam with material index (μ = 4, *l*/*h* = 10).

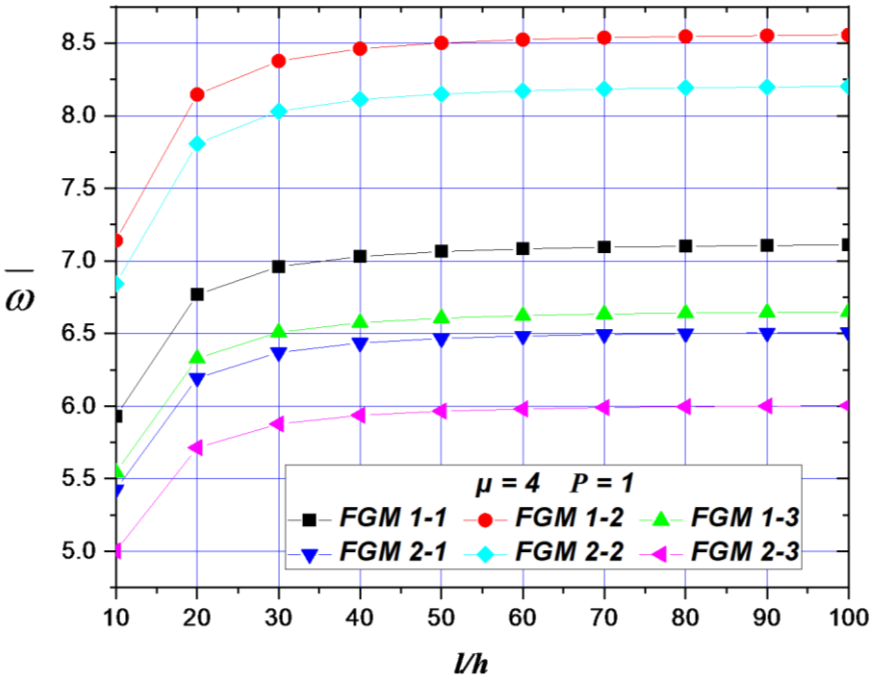

Figure 5. Variation of natural frequency of an FGM nano-beam with different length-to-thickness ratios and ceramic material combinations (P = 1, μ = 4).

8. Conclusions

This comprehensive parametric study and validation of four homogenization models advances our understanding of predicting the natural frequencies of functionally graded nano-beams. The results for varying length-to-thickness ratios, material indices and nonlocal parameters show excellent agreement across the Voigt, Tanka, Tamura and Reuss models. The relative difference in predicted natural frequencies between models decreases slightly as the length-to-thickness ratio increases. Furthermore, there are significant effects of the nonlocal parameter, material index and constitutive phases on the natural frequency. These findings provide justification that the validated computational homogenization techniques presented can reliably determine the natural frequencies of FGM nano-beams across a range of geometric and material parameters. Researchers can confidently utilize these models to gain new insights into the dynamic characteristics of nano-beams. The comprehensive parametric study and model validation represents an important advancement to the field by establishing these homogenization techniques as trusted tools for the design and analysis of nano-beams. This work elucidates the complex interplay between nano-beam dimensions, materials and intrinsic size effects, moving nano-scale research forward.

Use of AI tools declaration

The authors declare they have not used Artificial Intelligence (AI) tools in the creation of this article.

Conflict of interest

All authors declare no conflict of interest in this paper.

References

1. Eringen AC (1972) Nonlocal polar elastic continua. *Int J Eng Sci* 10: 1–16. https://doi.org/10.1016/0020–7225(72)90070–5
2. Eringen AC (1983) On differential equations of nonlocal elasticity and solutions of screw dislocation and surface waves. *J Appl Phys* 54: 4703–4710. https://doi.org/10.1063/1.332803
3. Eringen AC, Edelen DGB (1972) On nonlocal elasticity. *Int J Eng Sci* 10: 233–248. https://doi.org/10.1016/0020–7225(72)90039–0
4. Van VP, Tounsi A (2022) Free vibration analysis of functionally graded doubly curved nanoshells using nonlocal first-order shear deformation theory with variable nonlocal parameters. *Thin Wall Struct* 174: 109084. https://doi.org/10.1016/j.tws.2022.109084
5. Van VP, Van CN, Tounsi A (2022) Static bending and buckling analysis of bi-directional functionally graded porous plates using an improved first-order shear deformation theory and FEM. *Eur J Mech A-Solid* 96: 104743. https://doi.org/10.1016/j.euromechsol.2022.104743
6. Cuong LT, Nguyen KD, Le MH, et al. (2022) Nonlinear bending analysis of porous sigmoid FGM nanoplate via IGA and nonlocal strain gradient theory. *Adv Nano Res* 12: 441–455. https://doi.org/10.12989/anr.2022.12.5.441

7. Liu G, Wu S, Shahsavari D, et al. (2022) Dynamics of imperfect inhomogeneous nanoplate with exponentially-varying properties resting on viscoelastic foundation. *Eur J Mech A-Solid* 95: 104649. https://doi.org/10.1016/j.euromechsol.2022.104649
8. Faghidian SA, Tounsi A (2022) Dynamic characteristics of mixture unified gradient elastic nanobeams. *FU Mech Eng* 20: 539–552. https://doi.org/10.22190/FUME220703035F
9. Peddieson J, Buchanan GR, McNitt RP (2003) Application of nonlocal continuum models to nanotechnology. *In J Eng Sci* 41: 305–312. https://doi.org/10.1016/S0020–7225(02)00210–0
10. Xu M (2006) Free transverse vibrations of nano-to-micron scale beams. *P Roy Soc A-Math Phy* 462: 2977–2995. https://doi.org/10.1098/rspa.2006.1712
11. Billel R (2023) Contribution to study the effect of (Reuss, LRVE, Tamura) models on the axial and shear stress of sandwich FGM plate (Ti-6A1-4V/ZrO_2) subjected on linear and nonlinear thermal loads. *AIMS Mater Sci* 10: 26–39. https://doi.org/10.3934/matersci.2023002
12. Billel R (2022) Effect of the idealization models and thermal loads on deflection behavior of sandwich FGM plate. 2022 International Conference on Electrical Engineering and Photonics, 260–264. https://doi.org/0.1109/EExPolytech56308.2022.9950823
13. Rebai B, Mansouri K, Chitour M, et al. (2023) Effect of idealization models on deflection of functionally graded material (FGM) plate. *J Nano-Electron Phys* 15: 01022. https://doi.org/10.21272/jnep.15(1).01022
14. Reddy JN (2007) Nonlocal theories for bending, buckling and vibration of beams. *Int J Eng Sci* 45: 288–307. https://doi.org/10.1016/j.ijengsci.2007.04.004
15. Reddy JN, Pang SD (2008) Nonlocal continuum theories of beams for the analysis of carbon nanotubes. *J Appl Phys* 103: 023511. https://doi.org/10.1063/1.2833431
16. Zhang P, Schiavone P, Qing H (2023) Hygro-thermal vibration study of nanobeams on size-dependent visco-pasternak foundation via stress-driven nonlocal theory in conjunction with two-variable shear deformation assumption. *Compos Struct* 312: 116870. https://doi.org/10.1016/j.compstruct.2023.116870
17. Zhang P, Schiavone P, Qing H (2022) Two-phase local/nonlocal mixture models for buckling analysis of higher-order refined shear deformation beams under thermal effect. *Mech Adv Mater Struc* 29: 7605–7622. https://doi.org/10.1080/15376494.2021.2003489
18. Zhang P, Qing H (2022) Well-posed two-phase nonlocal integral models for free vibration of nanobeams in context with higher-order refined shear deformation theory. *J Vib Control* 28: 3808–3822. https://doi.org/10.1177/10775463211039902
19. Ebrahimi F, Barati MR, Zenkour AM (2017) Vibration analysis of smart embedded shear deformable nonhomogeneous piezoelectric nanoscale beams based on nonlocal elasticity theory. *Int J Aeronaut Space* 18: 255–269. https://doi.org/10.5139/IJASS.2017.18.2.255
20. Eltaher MA, Emam SA, Mahmoud FF (2012) Free vibration analysis of functionally graded size-dependent nanobeams. *App Math Comput* 218: 7406–7420. https://doi.org/10.1016/j.amc.2011.12.090
21. Nazemnezhad R, Hosseini-Hashemi S (2014) Nonlocal nonlinear free vibration of functionally graded nano-beams. *Compos Struct* 110: 192–199. https://doi.org/10.1016/j.compsruct.2013.12.006
22. Ebrahimi F, Barati MR, Civalek O (2020) Application of Chebyshev-Ritz method for static stability and vibration analysis of nonlocal microstructure-dependent nanostructures. *Eng Comput-Germany* 36: 953–964. https://doi.org/10.1007/s00366–019–00742–z

23. Hadji L, Avcar M (2021) Nonlocal free vibration analysis of porous FG nano-beams using hyperbolic shear deformation beam theory. *Adv Nano Res* 10: 281–293. https://doi.org/10.12989/anr.2021.10.3.281
24. Youcef G, Ahmed H, Abdelillah B, et al. (2020) Porosity-dependent free vibration analysis of FG nanobeam using non-local shear deformation and energy principle. *Adv Nano Res* 8: 37–47. https://doi.org/10.12989/anr.2020.8.1.037
25. Shariati A, Jung DW, Sedighi HM, et al. (2020). On the vibrations and stability of moving viscoelastic axiallyfunctionally graded nano-beams. *Materials* 13: 1707. https://doi.org/10.3390/ma13071707
26. Cornacchia F, Fabbrocino F, Fantuzzi N, et al. (2021) Analytical solution of cross-and angle-ply nano plates with strain gradient theory for linear vibrations and buckling. *Mech Adv Mater Struc* 28: 1201–1215. https://doi.org/10.1080/15376494.2019.1655613
27. Tocci MG, Fantuzzi N, Fabbrocino F, et al. (2021) Critical temperatures for vibrations and buckling of magneto-electro-elastic nonlocal strain gradient plates. *Nanomaterials* 11: 87. https://doi.org/10.3390/nano11010087
28. Luciano R, Darban H, Bartolomeo C, et al. (2020) Free flexural vibrations of nanobeams with non-classical boundary conditions using stress-driven nonlocal model. *Mech Res Commun* 107: 103536. https://doi.org/10.1016/j.mechrescom.2020.103536
29. Fabbrocino F, Funari MF, Greco F, et al. (2019) Dynamic crack growth based on moving mesh method. *Compos Part B-Eng* 174: 107053. https://doi.org/10.1016/j.compositesb.2019.107053
30. Fan F, Xu Y, Sahmani S, et al. (2020) Modified couple stress-based geometrically nonlinear oscillations of porous functionally graded microplates using NURBS-based isogeometric approach. *Comput Method Appl M* 372: 113400. https://doi.org/10.1016/j.cma.2020.113400
31. Hou F, Wu S, Moradi Z, et al. (2022) The computational modeling for the static analysis of axially functionally micro cylindrical imperfect beam applying the computer simulation. *Eng Comput-Germany* 38: 3217–3235. https://doi.org/10.1007/s00366–021–01456–x
32. Li L, Li XB, Hu YJ (2018) Nonlinear bending of a two-dimensionally functionally graded beam. *Compos Struct* 184: 1049–1061. https://doi.org/10.1016/j.compstruct.2017.10.087
33. Ye T, Qian D (2019) Nonlinear vibration analysis of a bi-directional functionally beam under hygro-thermal loads. *Compos Struct* 225: 111076. https://doi.org/10.1016/j.compstruct.2019.111076
34. Dehrouyeh-Semnani AM (2018) On the thermally induced non-linear response of functionally beams. *Int J Eng Sci* 125: 53–74. https://doi.org/10.1016/j.ijengsci.2017.12.001
35. Krysko AV, Awrejcewicz J, Pavlov SP, et al. (2017) Chaotic dynamics of the size-dependent non-linear micro-beam model. *Commun Nonlinear Sci* 50: 16–28. https://doi.org/10.1016/j.cnsns.2017.02.015
36. Eltaher MA, Fouda N, El-midany T, et al. (2018) Modified porosity model in analysis of functionally graded porous nano-beams. *J Braz Soc Mech Sci Eng* 40: 1–10. https://doi.org/10.1007/s40430–018–1065–0
37. Mirjavadi SS, Mohasel AB, Khezel M, et al. (2018) Nonlinear vibration and buckling of functionally graded porous nanoscaled beams. *J Braz Soc Mech Sci Eng* 40: 1–12. https://doi.org/10.1007/s40430–018–1272–8

38. Shafiei N, Mirjavadi SS, Afshari BM, et al. (2017) Vibration of two-dimensional imperfect functionally (2D-FG) porous nano-/micro-beams. *Comput Method Appl M* 322: 615–632. https://doi.org/10.1016/j.cma.2017.05.007
39. She GL, Yuan FG, Ren YR (2017) Thermal buckling and post-buckling analysis of functionally graded beams based on a general higher-order shear deformation theory. *Appl Math Model* 47: 340–357. https://doi.org/10.1016/j.apm.2017.03.014
40. Belarbi M, Houari M, Daikh AA, et al. (2021) Nonlocal finite element model for the bending and buckling analysis of functionally graded nano-beams using a novel shear deformation theory. *Composite Struct* 264: 113712. https://doi.org/10.1016/j.compstruct.2019.02.089
41. Akbaş ŞD, Dastjerdi S, Akgöz B, et al. (2021) Dynamic analysis of functionally graded porous microbeams under moving load. *Transp Porous Med* 142: 209–227. https://doi.org/10.1007/s11242–021–01686–z
42. Dang VH, Do QC (2021) Nonlinear vibration and stability of functionally graded porous microbeam under electrostatic actuation. *Arch Appl Mech* 91: 2301–2329. https://doi.org/10.1007/s00419–021–01884–7
43. Pham QH, Tran VK, Tran TT, et al. (2022) Dynamic instability of mag-netically embedded functionally porous nano-beams using the strain gradient theory. *Alex Eng J* 61: 10025–10044. https://doi.org/10.1016/j.aej.2022.03.007
44. Hosseini SA, Hamidi BA, Behrouzinia A (2022) A new model for non-linear vibration of functionally graded porous nano-beam based on non-local curvature and strain gradient tensors. *J Vib Control* 29: 4290–4301. https://doi.org/10.1177/10775463221114945
45. Nguyen DK, Nguyen KV, Dinh V, et al. (2018) Nonlinear bending of elasto-plastic functionally ceramic-metal beams subjected to nonuniform distributed loads. *Appl Math Comput* 333: 443–459. https://doi.org/10.1016/j.amc.2018.03.100
46. Wu Q, Qi G (2021) Quantum dynamics for Al-doped graphene composite sheet under hydrogen atom impact. *Appl Math Model* 90: 1120–1129. https://doi.org/10.1016/j.apm.2020.10.025
47. Wu Q, Yao M, Li M, et al. (2020) Nonlinear coupling vibrations of graphene composite laminated sheets impacted by particles. *Appl Math Model* 93: 75–88. https://doi.org/10.1016/j.apm.2020.12.008
48. Wu Q, Yao M, Niu Y (2022) Nonplanar free and forced vibrations of an imperfect nanobeam employing nonlocal strain gradient theory. *Commun Nonlinear Sci* 114: 106692. https://doi.org/10.1016/j.cnsns.2022.106692
49. Karami B, Shahsavari D, Janghorban M, et al. (2019) Resonance behavior of functionally graded polymer composite nanoplates reinforced with graphene nanoplatelets. *Int J Mech Sci* 156: 94–105. https://doi.org/10.1016/j.ijmecsci.2019.03.036
50. Voigt W (1889) Ueber die Beziehung zwischen den beiden Elasticitätsconstanten isotroper Körper. *Ann Phys-Berlin* 274: 573–587. https://doi.org/10.1002/andp.18892741206
51. Reuß A (1929) Berechnung der fließgrenze von mischkristallen auf grund der plastizitätsbedingung für einkristalle. *Z Angew Math Mech* 9: 49–58. https://doi.org/10.1002/zamm.19290090104
52. Gasik MM, Lilius RR (1994) Evaluation of properties of W/Cu functional gradient materials by micromechanical model. *Comp Mater Sci* 3: 41–49. https://doi.org/10.1016/0927–0256(94)90151–1

53. Zuiker JR (1995) Functionally graded materials: Choice of micromechanics model and limitations in property variation. *Compos Eng* 5: 807–819. https://doi.org/10.1016/0961–9526(95)00031–H
54. Tamura I, Tomota Y, Ozawa M (1973) Strength and ductility of Fe-Ni-C alloys composed of austenite and martensite with various strength. *Proc Third Int Conf Strength Met Alloy* 3: 611–615.
55. Mori T, Tanaka K (1973) Average stress in matrix and average elastic energy of materials with misfitting inclusions. *Acta Metall* 21: 571–574. https://doi.org/10.1016/0001–6160(73)90064–3
56. Belabed Z, Houari MSA, Tounsi A, et al. (2014) An efficient and simple higher order shear and normal deformation theory for functionally graded material (FGM) plates. *Compos Part B-Eng* 60: 274–283. https://doi.org/10.1016/j.compositesb.2013.12.057
57. Valizadeh N, Natarajan S, Gonzalez-Estrada OA, et al. (2013) NURBS-based finite element analysis of functionally graded plates: Static bending, vibration, buckling and flutter. *Compos Struct* 99: 309–326. https://doi.org/10.1016/j.compstruct.2012.11.008
58. Cheng ZQ, Batra RC (2000) Three-dimensional thermoelastic deformations of a functionally graded elliptic plate. *Compos Eng* 31: 97–106. https://doi.org/10.1016/S1359–8368(99)00069–4
59. Zemri A, Houari MSA, Bousahla AA, et al. (2015) A mechanical response of functionally graded nanoscale beam: An assessment of a refined nonlocal shear deformation theory beam theory. *Struct Eng Mech* 54: 693–710. https://doi.org/10.12989/SEM.2015.54.4.693

AIMS Press